Interfacial structure and electrical properties of ultrathin HfO_2 dielectric films on Si substrates by surface sol–gel method

2009 J. Phys. D: Appl. Phys. 42 015405

(http://iopscience.iop.org/0022-3727/42/1/015405)

IOP PUBLISHING JOURNAL OF PHYSICS D: APPLIED PHYSICS

J. Phys. D: Appl. Phys. **42** (2009) 015405 (5pp) doi:10.1088/0022-3727/42/1/015405

Interfacial structure and electrical properties of ultrathin HfO_2 dielectric films on Si substrates by surface sol–gel method

You-Pin Gong, Ai-Dong Li, Xu Qian, Chao Zhao and Di Wu

National Laboratory of Solid State Microstructures, Materials Science and Engineering Department, Nanjing University, Nanjing 210093, People's Republic China

E-mail: adli@netra.nju.edu.cn

Received 4 July 2008, in final form 3 November 2008
Published 4 December 2008
Online at stacks.iop.org/JPhysD/42/015405

Abstract

Ultrathin HfO_2 films with about ~3 nm thickness were deposited on n-type (1 0 0) silicon substrates using hafnium chloride ($HfCl_4$) source by the surface sol–gel method and post-deposition annealing (PDA). The interfacial structure and electrical properties of ultrathin HfO_2 films were investigated. The HfO_2 films show amorphous structures and smooth surface morphologies with a very thin interfacial oxide layer of ~0.5 nm and small surface roughness (~0.45 nm). The 500 °C PDA treatment forms stronger Hf–O bonds, leading to passivated traps, and the interfacial layer is mainly Hf silicate ($Hf_xSi_yO_z$). Equivalent oxide thickness of around 0.84 nm of HfO_2/Si has been obtained with a leakage current density of 0.7 A cm^{-2} at V_{fb} + 1 V after 500 °C PDA. It was found that the current conduction mechanism of HfO_2/Si varied from Schottky–Richardson emission to Fowler–Nordheim tunnelling at an applied higher positive voltage due to the activated partial traps remaining in the ultrathin HfO_2 films.

(Some figures in this article are in colour only in the electronic version)

1. Introduction

The scaling of silicon-based microelectronics devices has led to large leakage current of the silicon dioxide layer as a gate dielectric. It is necessary to replace the SiO_2 with high dielectric constant (k) oxides [1–5]. HfO_2 is a good candidate for applications in next generation metal-oxide-semiconductor devices due to a relatively high dielectric constant (k = 20–25) and a wide energy band gap (E_g ~ 5.6 eV) [6, 7]. In recent years, a number of methods have been investigated as routes for the fabrication of HfO_2 films, including atomic layer deposition (ALD) [8, 9], metal organic chemical vapour deposition [10, 11], magnetron sputtering deposition [12, 13] and pulsed laser deposition [14, 15]. However, most methods need expensive equipment for film deposition on heated substrates under vacuum conditions. The surface sol–gel technique is a stepwise film growth technique using consecutive surface reactions in a solution that resemble the self-limiting reaction in ALD, and it generally consists of four steps: nonaqueous chemisorption, rinsing, aqueous hydrolysis and drying [16]. Compared with ALD, the surface sol–gel is a fully solution-based technique and it can utilize inexpensive facilities with low operating costs to achieve precise thickness control of metal oxide films with nanometre precision. Some work has been reported that ultrathin films of conventional dielectric materials MO_2 (M = Ti, Zr) as well as their binary oxide composites MO_2–$M'O_2$ (M' = Ta, La) can be fabricated with dielectric properties comparable to those obtained by ALD or other vapour-deposition methods [16, 17]. But until now, the literature on electrical properties such as equivalent oxide thickness (EOT) and leakage current density of high k ultrathin films derived by the solution-based method is still very scarce.

In this paper, ultrathin HfO_2 films were fabricated on silicon substrates by the surface sol–gel process and post-deposition annealing (PDA). The interfacial structure, surface morphology and electrical properties of ultrathin HfO_2 films without and with PDA have been investigated in depth. The

voltage-dependent current conduction mechanism of ultrathin HfO_2 films was discussed.

2. Experiment

The substrates were n-type Si (1 0 0), cleaned by a standard RCA technique to remove organic and metallic contaminants on the wafer surface. Then the native silicon oxide layer on the surface was removed by immersion in a buffered HF solution ($HF : H_2O = 1 : 10$) for 5 min followed by rinsing in deionized water for 3 min to get a hydrogen-terminated Si wafer. Finally, to obtain a hydroxyl-terminated Si wafer, these hydrogen-terminated ones were ultrasonically cleaned in a 30% H_2O_2 solution for 10 min at 60 °C.

The precursor used was hafnium chloride ($HfCl_4$) with purity above 98%. The precursor solution (0.2 mol l^{-1}) was obtained by dissolving $HfCl_4$ in 1 : 9 (v/v) acetylacetone/ethanol in a N_2 glovebox. The OH-terminated Si was immersed in the hafnium precursor solution for 3 min, followed by rinsing in ethanol for 1 min, hydrolyzed in deionized water for 3 min and finally dried by N_2 gas flow, thus completing one cycle. The deposition was repeated for 50 cycles. PDA of ultrathin HfO_2 films was performed at 500 °C for 5 min by rapid thermal annealing (RTA) in nitrogen atmosphere to remove the residual impurity of the as-deposited HfO_2 films and further densify the oxide films. Metal–insulator–semiconductor capacitors were fabricated by sputtering Pt top electrodes through a shadow mask with a diameter of 200 μm for electrical measurements.

Microstructural and interfacial structures of ultrathin HfO_2 films were characterized by high-resolution transmission electron microscopy ((HRTEM) Tecnai F20 S-Twin, FEI), x-ray photoelectron spectroscopy ((XPS) ESCALB MK-II). The surface roughness was examined using tapping mode with a scan step of 2 nm by atomic force microscopy ((AFM) NTEGRA Spectra, NT-MDT). The film roughness was represented by the root mean square value (RMS) in a $1 \times 1\,\mu m^2$ area. Capacitance–voltage (C–V) and leakage current density–voltage (J–V) characteristics were measured by a precise impedance analyzer (Agilent 4294A) and a PA-meter (HP 4140B) voltage source.

3. Results and discussion

For ultrathin gate dielectrics oxide of several nanometres, the surface uniformity becomes more stringent for oxide reliability issues. Figure 1(a) shows the AFM image of HfO_2 ultrathin films derived by surface sol–gel. A small surface roughness with a RMS of ~0.45 nm was obtained. Figure 1(b) shows the typical cross-sectional HRTEM image of HfO_2 ultrathin films deposited on Si substrates and annealed at 500 °C in N_2. Obviously, the samples exhibit an amorphous structure with about ~3 nm thickness. The parasitic oxide interfacial layer (IL) of the HfO_2 film is thinner than 0.5 nm. The IL of SiO_x or Hf silicate easily appeared during the deposition process, because before the deposition, the Si substrates were dipped in a 30% H_2O_2 solution to form a hydroxyl-terminated Si surface. In addition, in most of the literature, it has been found that the crystallinity of HfO_2 films is related to the film

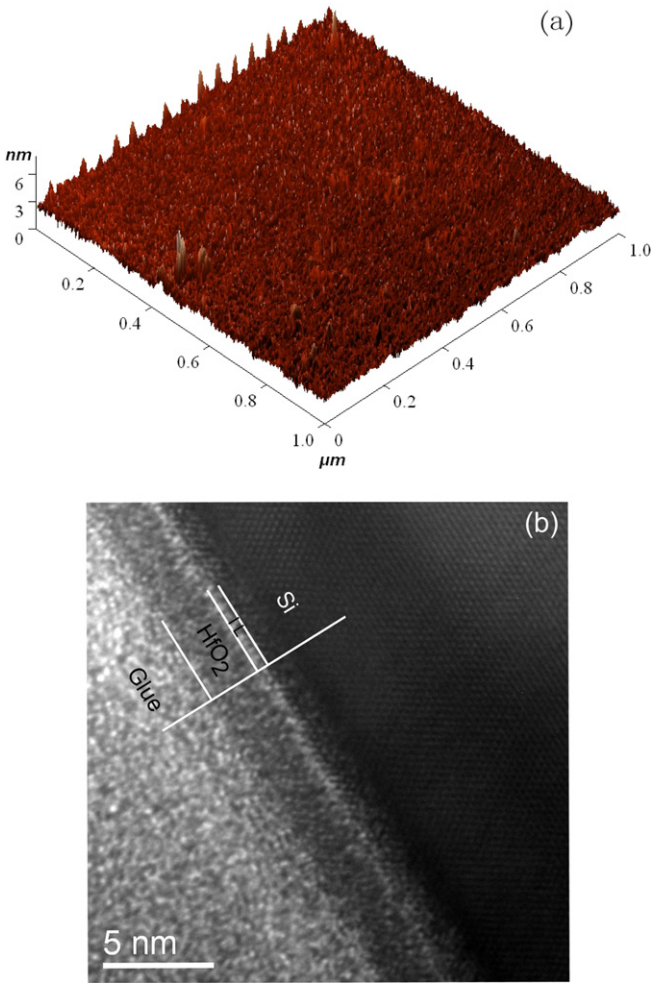

Figure 1. (a) The three-dimensional AFM and (b) cross-sectional HRTEM images of HfO_2 ultrathin films with 500 °C PDA treatment.

thickness. Generally, the HfO_2 films with a thickness below ~5 nm show an amorphous structure even if annealed at a high temperature [18]. Our result also confirms the conclusion.

In order to further reveal the interfacial structure, XPS analyses were used to analyse the composition and chemical bond of HfO_2 ultrathin films on Si without and with PDA. Based on the signal position and intensity of Hf and Si, the interfacial status of the thin film can be deduced. The binding energy of core levels was calibrated by setting the carbon 1s peak at 284.6 eV. Figure 2(a) shows the Hf 4f region of the XPS spectra which consists of the $4f_{5/2}$ and $4f_{7/2}$ components at different binding energies of Hf–O bonds. The Hf $4f_{5/2}$ and Hf $4f_{7/2}$ features for the as-deposited HfO_2 film are 18.2 eV and 16.8 eV, respectively. And the spin–orbit splitting is ~1.4 eV, which is familiar in the Hf–O reference spectra (1.5 eV), consistent with the literature data of dielectric HfO_2/Si [19, 20]. These results indicate that the HfO_2 film has been formed. It is noteworthy that the binding energies of $4f_{5/2}$ and $4f_{7/2}$ increase to 18.7 and 17.2 eV after PDA treatment, implying that more Hf elements were oxidized from a low oxidation state to a high oxidation state during PDA. That is to say, the 500 °C PDA treatment forms stronger Hf–O bonds, leading to passivated traps [21, 22]. This will improve the leakage properties of ultrathin HfO_2 films.

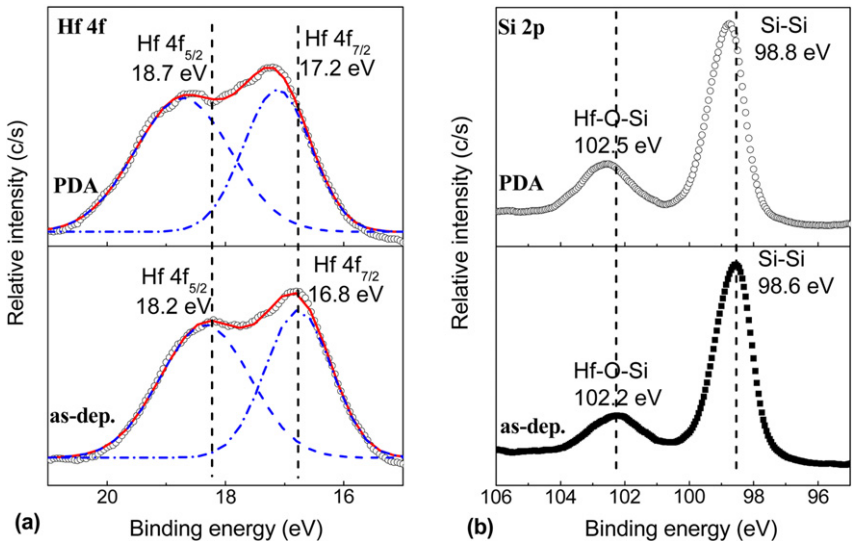

Figure 2. (*a*) Hf 4f and (*b*) Si 2p regions XPS spectra of HfO_2 ultrathin films deposited on Si with and without 500 °C PDA treatment.

Figure 2(*b*) shows XPS Si 2p spectra of the HfO_2 films without and with PDA treatment. The right peaks near ∼98.7 eV for both films indicate the Si 2p signal as Si–Si bonding from the substrate. Jin *et al* have reported that the intensity in the region around 102–102.7 eV originates from the Hf silicate film and is associated with the Hf–O–Si bond, while the intensity in the region 102.7–104 eV is associated with the Si–O–Si bond [23]. From figure 2(*b*), the left peaks for the as-deposited and PDA treated ultrathin HfO_2 films were ∼102.2 eV and∼102.5 eV, respectively, which is associated with Hf–O–Si from the Hf silicate IL ($Hf_xSi_yO_z$). It can be seen that after PDA treatment, the left peak of the Si2p signal shifts slightly to the higher binding energy with enhanced signal, indicating the diffusion of the Si element in the IL. In addition, the element chlorine was not detected within the detectable limit, which implies low chlorine residue in ultrathin HfO_2 films.

The *C*–*V* curves of Pt/HfO_2/Si structures with and without 500 °C PDA treatment were measured at frequencies of 500 kHz and 1 MHz, respectively. Figure 3 shows the actual frequency-independent capacitance. The true capacitance can be calculated from the measured capacitance at two different measuring frequencies with quantum mechanical correction according to the theory by Yang so as to remove the effect of leakage current [24]. Setting the frequencies as f_1 and f_2, and the corresponding MOS capacitance as C_1 and C_2, we can get the actual capacitance:

$$C_{\text{actual}} = \frac{C_1 f_1^2 - C_2 f_2^2}{f_1^2 - f_2^2}. \quad (1)$$

As we know $C = (\varepsilon_0 \times \varepsilon_r \times A)/t$, the EOT can be estimated from these accumulation capacitances in the calculated *C*–*V* curve by using a simple formula (2):

$$\text{EOT} = (\varepsilon_0 \times \varepsilon_{SiO_2} \times A)/C_{\text{actual}}, \quad (2)$$

where ε_0 is the vacuum dielectric constant and *A* is the capacity area. As-deposited films exhibit an EOT value of 1.24 nm

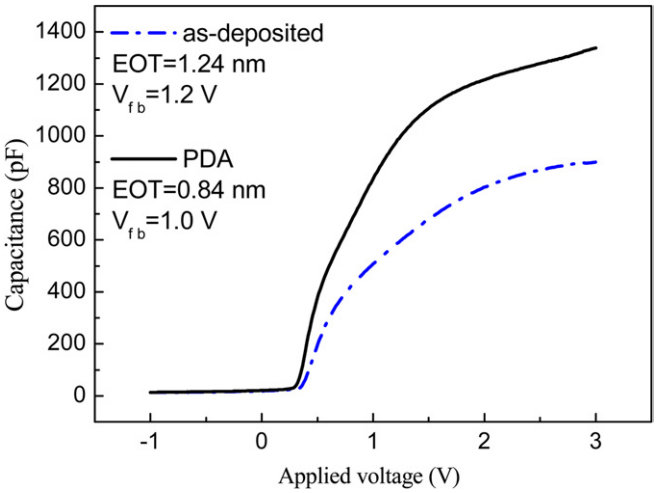

Figure 3. Capacitance–voltage (*C*–*V*) characteristics of Pt/HfO_2/Si structures with and without 500 °C PDA treatment.

with the flatband voltage (V_{fb}) of 1.2 V. After 500 °C PDA, the EOT value of 0.84 nm was achieved with the flatband voltage (V_{fb}) of 1.0 V for the Pt/HfO_2/Si capacitor, and it is a very low EOT value reported to date for HfO_2 fabricated by other methods. The reduced EOT value of the PDA treated HfO_2 film is attributed mainly to the improved film density and removal of some impurity in the film. The dielectric constant of the HfO_2 film was estimated to be about 14 by using a simple formula: $k = T_{\text{high-}k}(\varepsilon_{SiO_2}/\text{EOT})$, where $T_{\text{high-}k}$ is the physical thickness of the HfO_2 film with a value of 3 nm (figure 1), ε_{SiO_2} of permittivity of SiO_2 with a value of 3.9 and EOT of 0.84 nm. The calculated lower permittivity of HfO_2 could be attributed to the presence of the IL (Hf silicate).

The leakage current densities (*J*) as a function of the applied voltage (*V*) of HfO_2 films are described in figure 4. The as-deposited HfO_2 film exhibits larger leakage current ($J = 2.3\,\text{A cm}^{-2}$ at $V_{fb} + 1$ V) because of the existence of numerous traps and some impurity. The interfacial properties have an important influence on the leakage current density [25].

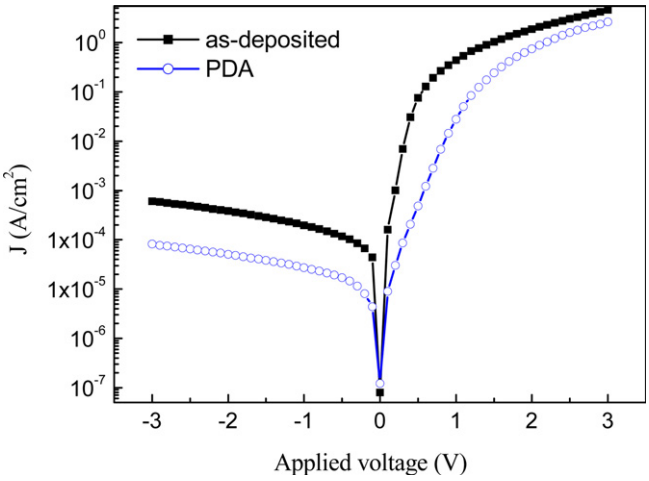

Figure 4. Leakage current densities–voltage (J–V) characteristics of Pt/HfO_2/Si structures with and without 500 °C PDA treatment.

The leakage current ($J = 0.7\,\mathrm{A\,cm^{-2}}$ at $V_{fb} + 1\,\mathrm{V}$) was suppressed after PDA at 500 °C in N_2 due to the passivation of interfacial states during PDA treatment.

To further understand the behaviour of leakage current, the current conduction mechanism of ultrathin HfO_2 films was investigated. Figure 5(*a*) plots $\ln(J/V)$ versus the square root of the applied voltage ($V^{1/2}$) for the as-deposited HfO_2 film. A good linear fitting appears while the applied positive voltage is higher than 1 V. This indicates that Poole–Frenkel (PF) emission predominates in the leakage current of the as-deposited HfO_2 film. PF emission is a bulk-limited conduction process, which is field-assisted thermal detrapping of carriers from the bulk oxide into the conduction band [22, 26], as schematically described in the inset of figure 5(*a*). The plot of $\ln(J)$ versus the square root of the applied voltage ($V^{1/2}$) for the PDA treated HfO_2 film is given in figure 5(*b*). When the applied positive voltage is lower than 1.2 V, the linear trend indicates that the current conduction mechanism is Schottky–Richardson (SR) emission, which is a thermionic emission of an electron jump over a surface barrier [26] (inset of figure 5(*b*)). The conversion of the current conduction mechanism from PF emission to SR emission demonstrates theoretically that partial traps were terminated after annealing at 500 °C in N_2. However, with increasing applied voltage, the partial traps remaining in the HfO_2 film were activated resulting in Fowler–Nordheim (FN) tunnelling [27] (figure 5(*c*)). The inset in figure 5(*c*) shows a schematic energy-band diagram to explain trap-assisted tunnelling. The leakage current density increases rapidly under a higher positive applied voltage due to the current conduction mechanism changing from SR emission to FN tunnelling.

4. Conclusion

Ultrathin HfO_2 films were prepared on n-type (1 0 0) Si substrates by surface sol–gel process. A series of analytical techniques were used to characterize the structure, surface morphology and electrical properties of ultrathin HfO_2 films on Si. The HfO_2 films have amorphous structures with a very thin IL of ∼0.5 nm and small surface roughness (∼0.45 nm).

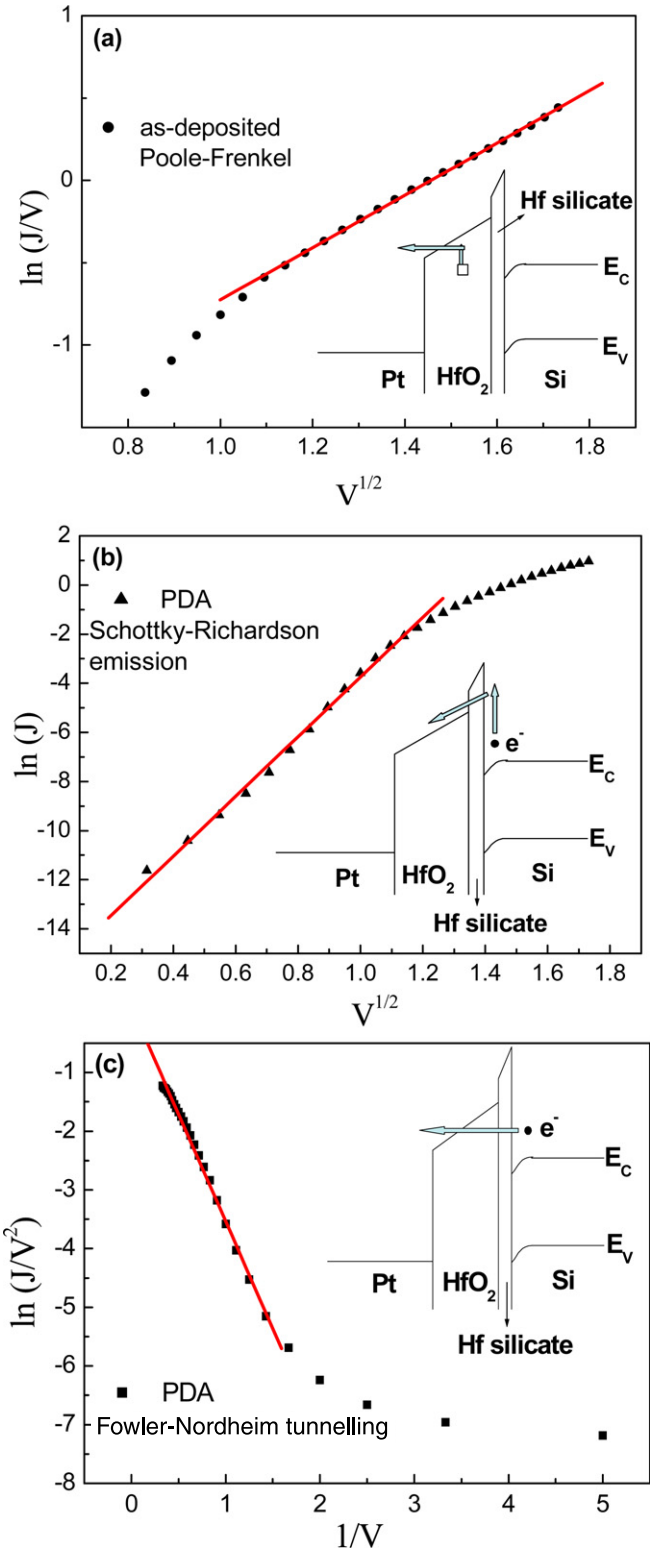

Figure 5. (*a*) The curve of $\ln(J/V)$ versus square root of the positive applied voltage ($V^{1/2}$) for the as-deposited HfO_2 film; (*b*) the curve of $\ln(J)$ versus square root of the positive applied voltage ($V^{1/2}$) for the PDA treated HfO_2 film; (*c*) the curve of $\ln(J/V^2)$ versus reciprocal of positive applied voltage ($1/V$) for the PDA treated HfO_2 film. The insets in (*a*), (*b*) and (*c*) show a schematic energy-band diagram to describe the PF emission, SR emission and FN tunnelling, respectively.

XPS analyses indicate that the 500 °C PDA treatment forms stronger Hf–O bonds, leading to passivated traps, and the IL is mainly Hf silicate ($Hf_xSi_yO_z$) between HfO_2 and Si. The EOT value of 0.84 nm has been obtained, which is a very low EOT value reported to date for HfO_2 fabricated by other methods. For Pt/HfO_2/Si after 500 °C PDA treatment, the leakage current density is 0.7 A cm^{-2} at $V_{fb} + 1$ V. It was found that the current conduction mechanism varied from Schottky–Richardson emission to Fowler–Nordheim tunnelling at an applied higher positive voltage due to the activated partial traps remaining in the HfO_2 films.

Acknowledgments

This project is supported by the Program for New Century Excellent Talents in University (NCET-04-0451). It was also partially supported by the Natural Science Foundation of China and Jiangsu Province (50672036, 10704035 and BK2006122) and a grant for the State Key Program for Basic Research of China (2006CB921805 and 2009CB929503).

References

[1] Kingon A I, Maria J P and Streiffer S K 2000 *Nature* **406** 1033
[2] Robertson J 2006 *Rep. Prog. Phys.* **69** 327
[3] Martínez F L, Toledano-Luque M, Gandía J J, Cárabe J, Bohne W, Röhrich J, Strub E and Mártil I 2007 *J. Phys. D: Appl. Phys.* **40** 5256
[4] Govindarajan S, Böscke T S, Sivasubramani P, Kirsch P D, Lee B H, Tseng H-H and Jammy R 2007 *Appl. Phys. Lett.* **91** 062906
[5] Ribes G, Mitard J, Denais M, Bruyere S, Monsieur F, Parthasarathy C, Vincent E and Ghibaudo G 2005 *IEEE Trans. Device Mater. Reliab.* **5** 5
[6] Tang C, Tuttle B and Ramprasad R 2007 *Phys. Rev.* B **76** 073306
[7] Adelmann C, Sriramkumar V, Elshocht S V, Lehnen P, Conard T and Gendt S De 2007 *Appl. Phys. Lett.* **91** 162902
[8] Chen R, Kim H, McIntyre P C and Bent S F 2005 *Chem. Mater.* **17** 536
[9] Maikap S, Lee H Y, Wang T-Y, Tzeng P-J, Wang C C, Lee L S, Liu K C, Yang J-R and Tsai M-J 2007 *Semicond. Sci. Technol.* **22** 884
[10] Yang T S *et al* 2005 *Chem. Mater.* **17** 6713
[11] Abermann S, Pozzovivo G, Kuzmik J, Strasser G, Pogany D, Carlin J-F, Grandjean N and Bertagnolli E 2007 *Semicond. Sci. Technol.* **22** 1272
[12] Liu X and Li D J 2006 *Appl. Surf. Sci.* **253** 2143
[13] Roy A, Dhar A, Bhattacharya D and Ray S K 2008 *J. Phys. D: Appl. Phys.* **41** 095408
[14] Conley J F, Ono Y, Tweet D J and Solanki R 2004 *Appl. Phys. Lett.* **84** 398
[15] Ratzke M, Wolfframm D, Kappa M, Kouteva-Arguirova S and Reif J 2005 *Appl. Surf. Sci.* **247** 128
[16] Aoki Y, Kunitake T and Nakao A 2005 *Chem. Mater.* **17** 450
[17] Aoki Y and Kunitake T 2004 *Adv. Mater.* **16** 118
[18] Cho M-H, Roh Y S, Whang C N, Jeong K, Nahm S W, Ko D-H, Lee J H, Lee N I and Fujihara K 2002 *Appl. Phys. Lett.* **81** 472
[19] Sayan S, Garfunkel E, Nishimura T, Schulte W H, Gustafsson T and Wilk G D 2003 *J. Appl. Phys.* **94** 928
[20] Maida O, Fukayama K, Takahashi M, Kobayashi H, Kim Y-B, Kim H-C and Choi D-K 2006 *Appl. Phys. Lett.* **89** 122112
[21] Hong J-H, Moon T-H and Myoung J-M 2004 *Microelectron. Eng.* **75** 263
[22] Tsai C-T, Chang T-C, Kin K-T, Liu P-T, Yang P-Y, Weng C-F and Huang F-S 2008 *J. Appl. Phys.* **103** 074108
[23] Jin H, Oh S K, Cho Y J, Kang H J and Tougaard S 2007 *J. Appl. Phys.* **102** 053709
[24] Yang K J and Hu C M 1999 *IEEE Trans. Electron Devices* **46** 1500
[25] Puthenkovilakam R, Sawkar M and Chang J P 2005 *Appl. Phys. Lett.* **86** 202902
[26] Cheong K Y, Moon J H, Kim H J, Bahng W and Kim N-K 2008 *J. Appl. Phys.* **103** 084113
[27] Rosenbaum E and Register L F 1997 *IEEE Trans. Electron Devices* **44** 317